Proceedings of the Second Jordanian Geological Conference. Amman - April 1985 (68 - 174)

ON THE GEOMETRY OF STRATA-BOUND Fe,Cu,Zn AND Pb SULPHIDES IN THE METAPYROCLASTICS AT UM SAMIUKI AREA, EASTERN DESERT, EGYPT

Mortada Mourad El Aref
Dept of Geology,
Cairo University
Egypt.

Ali Khudeir, and Galal Hamed El Habaak
Dept of Geology,
Assiut University
Egypt.

ABSTRACT

Strata-bound to stratiform Fe, Cu, Zn and Pb. sulphide deposits occur in late Proterozoic, weakly metamorphosed volcanic association at Um Samiuki area, Eastern Desert, Egypt. The enclosing metavolcanic association is constituted of bedded pyroclastics intercalated with abundant volcanic sheets. The metapyroclastics are essentially composed of subaquous, massive and banded metadacite and meta-andesite tuffs. The volcanic intercalations are represented by meta-andesites, metadacites and metabasalts, metarhyolites are rare.

The sulphide minerals are confined to the banded tuffs. Systematic megascopic and microscopic study of the distribution patterns of the sulphide minerals revealed symmetric relations with the primary and deformational sedimentary fabrics of the enclosing banded tuffs suggesting syngenetic origin.

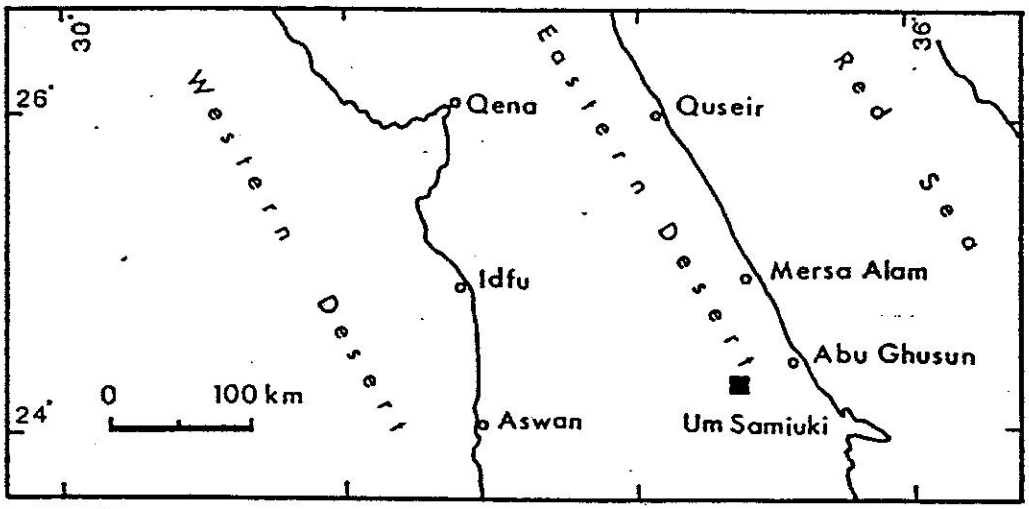

Fig. 1 Location map of Um Samiuki mine area

INTRODUCTION

Um Samiuki area is located in the southern part of the basement complex of Egypt (Fig.1). It is bounded by the following coordinates:

Lat. 24° 40' and 24° 26'N
Long. 34° 37' and 35° 00 E

The area underconsideration is mainly covered by volcanic/ volcaniclastic rocks of late Proterozoic age and is characterized by the occurrence of massive Fe, Cu, Zn and Pb sulphide deposits encountared in some mines and prospects scattered in an area of about 100 km^2.

The geology of Um Samiuki area and the occurring sulphide deposits have been investigated by several authors including: BALL (1912) HUME (1937), El SHAZLY (1957,1969), El SHAZLY and AFIA (1958), GARSON and SHALABY (1976), SEARLE et al. (1976 a and b), HUSSEIN et al. (1977), SHUKRI and MANSOUR (1980), SOLIMAN (1981) and HAFEZ and SHALABY (1983).

HUME (1937) considered that the mineralization at Um Samiuki is intimately connected with diabasic and ultrabasic dykes. EL SHAZLY and AFIA (1958) suggested that the polymetallic sulphide association of Um Samiuki was formed by hydrothermal replacement of low mesothermal stage along shear zones. The authors believed that the source of the hydrothermal soultions is related to Late Precambrian granitic activities. SEARLE et al (1976 a) described the ore as massive sulphide type of volcanogenic origin that has been formed by acidic volcanisms. HUSSEIN et al (1977) showed that the Um Samiuki ore is a syngenetic volcanogenic sedimentary deposit that has formed on the sea floor, probably from a submarine exhalative source. SOLIMAN (1981) described the ore deposits at Um Samiuki as a stratiform type syngenetically formed within felsic metavolcanics. He thought that the ore minerals were depositedd in a submarine environment above a submarine volcanic vent system at the interface between the metavolcanic rocks and the sea water.

The present paper is an attempt to clarify the origin of the sulphide deposits of Um Samiuki by studing systematically and in detail the geometry and distribution patterns of the ore minerals in low to high grade massive ores and from the scale of the field

down to microscopic interfaces. The observed geometric interrelationships gave inductive informations about place, time of formation and sequence of crystallization of the sulphide ore minerals. They showed clearly that the sulphides were deposited syngenetically during diagenesis within pyroclastic sediments under submarine conditions.

VOLCANIC AND VOLCANICLASTIC COUNTRY ROCKS

Field and petrographic examinations revealed that Um Samiuki area is covered mainly by a thick succession of submarine volcanic and volcaniclastic rocks (Pl.I, Fig.a). This succession was considered a part of the geosynclinal Shadli metavolcanics (EL SHAZLY, 1964 and EL RAMLY, 1972) but were separated recently as Um Samiuki Formation (SEARLE et al, 1976b) having island arc characters (GARSON and SHALABY, 1976; HAFEZ and SHALABY, 1983).

The volcanic rocks are represented mainly by a repetition of sheet flow lavas of calc-alkaline composition including the following rock types arranged according to their abundance: andesite, dacite, basalt and rhyodacite. Volcanics of rhyolitic composition are very rare. Pillow structures and vesicular textures are the common fabrics characterizing these sheet flows (Pl. I, Fig. b). Volcaniclastics, mainly pyroclastics, are more abundant than the volcanics and occur as conformable, massive and laminated beds of variable thicknesses. The pyroclastics are predominately of andesite and dacite composition. They include the following rock types differentiated according to grain-size and fabrics into (a) volcanic breccia (Pl.I,Fig.c) and pillow breccia, (b) agglomerates having isotropic or network fabric, and (c) stratified and laminated lapilli tuffs, tuffs and dust tuffs interbanded with chert and calcareous bands or nodules (Pl.I, Fig.d). Pyrite-rich laminae or bands are frequently observed intercalating coarse and medium grained tuffs (Pl. I, Fig.e). The tuffs commonly exhibit well pronounced penecontemporaneous deformational features recognized in handpacimens and thin sections. They comprise the following structures:

1. Downwards convexity of coarse-grained bands or laminae into finer grained underlying horizons (Pl.I,Fig.f & Pl.II,Fig.a).

2. Load cast or geopetal loading developed by downward protrusion of coarse lithic or crystal fragments into underlying fine-grained bands or laminae (Pl.II,Figs.b & c).

3. Load balls and pillow structures characterizing the lower portions of coarse to medium-grained tuff bands resting on finer-grained tuff, cherty or calcareous bands or laminae.

4. Cut and fill structure evolved through filling of small erosional chanells on the upper surfaces of lower bands by depositional materials of the upper layers (Pl. II, Fig. d).

5. Convolute bedding and contorted lamination usually confined within certain stratigraphic units.

6. Synsedimentary slumping and related small scale folds and faults. Slumping structure may affect several bands or laminae embedded between undisturbed upper and lower horizons (Pl. II, Fig. e).

The formation of calcareous and chert nodules and their coalescence into continuous bands suggest preconsolidation chemical rearrangement.

Petrographically, the tuffs are composed of varying proportions of lithic and crystal fragments embedded in a fine-grained groundmass composed of dust-size ashes and silicious, calcareous and clayey material. The lithic fragments are predominately of andesite composition, while the crystal ashes are represented mainly by plagioclase (An 30-36) and quartz together with subordinate amounts of pyroxenes, glass shards are sometimes present. The groundmass of the coarse to medium-grained tuff varieties are noticeably characterized by the presence of organic carbonaceous debris. The carbonaceous materials from long streaks usually arranged parallel or subparallel to the original lamination of the enclosing rocks. Organic carbon content of four tuff samples, two of which containing sulphides, was determined by the chromic acid method (JACKSON, 1958) and was found to range between 0.2% to 0.4%.

The studied tuffs were subjected to postdepositional compaction and lithification processes. Segregation, cementation, recrystallization and replacement appear to be the main processes affecting the rocks during the time of burial and before final consolidation. Formation of calcareous and chert nodules may be due to chemical segregation. Cementation has been achieved through (a) precipitation and recrystallization of chalcedony (Pl. II, Fig.f) and carbonates (Pl. II, Fig.g), (b) formation of

authigenic chlorite and epidote (?), and (c) authigenic quartz and albite overgrowths around clastic quartz and feldspar grains (Pl. II, Fig.h). Authigenic albite and chlorite in submarine volcaniclastics are attributed to diagenesis (FISHER and SCHMINCKE, 1984). The authigenic albite overgrowths are commonly intergrown with quartz in a myrmekitic fashion. Quartz commonly replaces calcite and is less commonly replaced by calcite. Calcite embays locally idiomorphic pyrite crystals.

The volcanic and volcaniclastic rocks suffered very low-grade regional metamorphism whereby epidote, actinolite, tremolite and chlorite were formed on the expense of the original constituents. The metavolcanics were subjected locally to brecciation and intense hydrothermal alteration leading to the formation of talc-tremolite-dolomite-calcite assemblages. The Brecciation and talc formation were associated with mobilization and redeposition of chalcopyrite.

The occurrence of talc at Um Samiuki is attributed by EL SHAZLY and AFIA (1958) to the introduction of hydrothermal solutions along shear zones before the formation of the sulphides. Conversely, SEARLE et al (1976 a) and SOLIMAN (1981) suggest that a period of intensive magnesium metasomatism induced extensive replacement of footwall breccia, lapilli tuff and massive sulphides after the formation of the sulphide ore.

REGIONAL GEOMETRIC CHARACTERS OF THE SULPHIDES

The sulphides are confined to certain pyroclastic horizons within the Um Samiuki Formation. No primary sulphide minerals were ever found in the associated volcanic rocks. This manner of stratigraphic relation indicate that the sulphide deposits of Um Samiuki belong to the strata-bound type. Moreover, the sulphides exhibit well pronounced stratification characters symmetrically concordant with the original fabrics of the horst rocks. The sulphides of Um Samiuki are classified according to their paragenesis into two main geometric forms:

1) stratiform to strata-bound pyrite with or without sphalerite and chalcopyrite.

2) stratiform to strata-bound pyritic massive sulphides containing Fe, Zn, Cu and Pb sulphide minerals.

The second form is mainly localized in the mine sectors, whereas the first form is very common over wide areas throughout the same stratigraphic horizons around the mines.

MEGASCOPIC-MICROSCOPIC GEOMETRIC DESCRIPTION

Detailed investigation on the above mentioned sulphide forms have been carried out on oriented slabs, thin sections and polished sections to deduce the different geometric distribution patterns of the sulphides and their intimate relations with the primary and deformational fabrics of the host rocks. The identified geometric distribution types of the sulphides are schematically represented and systematically classified in Pl. III.

Group I (Pl. III) comprises pyrite spots, crystals or clusters, with or without sphalerite and chalcopyrite, arranged in stratiform (types Ia to Ie) or strata-bound (types I1 to I6) configurations. These types are mostly encountered within distinct thick to thin bands or even laminae of the pyroclastics (Pl. IV). Type Ia refers to dissiminated pyrite spots or dots (up to 100 in diameter) showing weak linear arrangement. In type Ib, the pyrite spots are distributed in stratified alignment. Type Ic shows stratified distribution of idiomorphic pyrite crystals (up to 1 mm in diameter). Type Id exhibits gradual lateral grouping or clustering of pyrite crystals forming irregularly thick bands or laminae, up to 1 cm in thickness transitional to the next type. Type Ie displays regular stratified thin bands or laminae of grouped pyrite crystals. The gradual transition from one type into the other reflects progressive crystal growth and accumulation during segregation process. In type I1, the dissiminated pyrite spots are arranged in a wavy pattern resembling convolution or crumbling structure (Pl. V, Fig.a). Types I2 and I3 exhibit geopetal loading structures developed by tuff clasts into convoluted, aligned patterns of pyrite spots (type I 2) or crystals (type I3 and Pl. V, Fig.b). The deformed types I1, I2 and I3 are enclosed within undisturbed tuff bands. Type I4 represents loaded laminae of dissiminated pyrite crystals showing symmetrical relationship with the asociated convoluted tuff laminae. In type I5, the lower surface of the segregated banded or laminated pyrite crystals show downward projection into underlaying sediments corresponding to load or cut and fill structures. Type I6 shows pyrit crystals dissipated along strata-bound cross cutting cracks probably related to small scale synsedimentary slump faults.

Group II (Pl. III) displays the geometric characters of the pyritic massive sulphide differentiated into stratiform and strata-bound patterns. The strata-bound types are believed to be related to preconsolidation to postconsolidation deformational processes. The vertical disposition of these types is based on the paragenesis of the sulphide minerals and their sequence of crystallization. The main recognized paragenetic associatios are: pyrite - sphalerite - chalcopyrite, pyrite - sphalerite - chalcopyrite - galena - fahlore and, sphalerite - chalcopyrite - galena - fahlore - bornite covellite. Type II a represents stratified pattern bounded by linear arrangement of pyrite crystals alternating within thin bands or laminae of sphalerite and chalcopyrite (Pl. V., Fig.c). In type II b, the stratified pattern is illustrated by cross-lamination distribution of pyrite crystals. Type II c is similar to type II a, but the alternating bands consist of sphalerite, chalcopyrite and galena. Type II d shows laminated massive sulphide lacking pyrite. The lamination fabric is indicated by horizontal arrangement of separate or interconnected elongate patches of chalcopyrite, galena and fahlore intercalating through a groundmass of sphalerite. These elongate patches range in thickness between several microns and few millimeters. Type II e is similar to type II d but differs by the first appearance of bornite and covellite. Strata-bound preconsolidational fabrics are represented by the development of typical loading, slumping and convolution structures. Loading structures are developed by the pressure of coarse pyrite crystals exerted onto underlaying sulphide laminae. Type II 1 represents slump structure indicated by lateral displacement and vertical sinking of pyrite crystals into interbedded sulphides of types IIa,IIb and .IIc. Fig.2 shows a detailed microscopic drawing of slump structure of type II1. Note the folding of the pyrite rich laminae and their dislocation along microfaults. The sulphide bands with slump structure are bounded by undisturbed upper and lower sulphide bands or laminae. Within the slumped bands, the fold axial planes exhibit a conformable orientation as the associated microfaults. The pyrite rich laminae are gradually folded then broken along microfaults. Slump structure is recorded in the massive Cu, Pb, Zn - Ag sulphide ore bodies of Colquijirca, Central Peru (LEHNE and AMSTUTZ, 1982). Types II 2 and II 3 exhibit undulated or convoluted pyrite-rich or sulphide laminae enclosed within the sphalerite. Types II A and II B represent strata-bound veinlets of chalcopyrite cutting across sulphides of types IIa, IIb and IIc (Pl.V,Fig.c). In Types IIC & IID, the sulphide patches intercalating the sphalerite base are interconnected by veinlets having the same composition.

The described patterns displayed by the sulphide minerals are identical to typical diagenetic sedimentary textures formed during burial and prior to final consolidation. They can be correlated with the typical sedimentary ore fabrics described by SCHULZ (1976). The low grade sulphide represented by pyrite, with or without sphalerite and chalcopyrite, shows the best conformable geometric relations with the fabrics of the enclosing volcaniclastic sediments. The same fabrics displayed by the pyrite are also well recognized in the massive sulphides of group II, suggesting progressive increase in the concentration of Cu, Zn and Pb sulphides in a more suitable environment. The strata-bound cross-cutting veinlets may be related to subsequent migration of chalcopyrite into synsedimentary fractures or cracks.

The strata-bound types IIE, IIF & IIG comprise fractured massive sulphide (types IIE & IIF) and sulphide breccia (type IIG). The fractures within the sulphides and the matrix between the sulphide breccia are mainly occupied by talc minerals, tremolite, dolomite and blocky calcite. The breccia fragments are composed mainly of sulphides of types IIa, IIb, IIc & IId together with subordinate volcanic rock fragments. The fragments are encrusted by a youger generation of chalcopyrite associated with the talc formation after the brecciation of the primary ore (Pl. V,Fig.d). Brecciation must have been accompanied by hydrothermal solutions that caused the development of talc tremolite and the mobilization of already present sulphide minerals, for example chalcopyrite.

MICROSCOPIC GEOMETRIC INTERFACES

The contact relations (intergrowth index) of the different mineral constitutes of the above described geometric types have been studied. Automorphic outlines and concave-convex interfaces are the main geometric parameters characterizing the contact relations between the studied sulphides and the gangue and between the sulphide minerals themselves. Considering the fact that in the case of free growth, the interface between solid and melt, solution or gas, may be regarded as a surface and in many instances true surface tensions operate giving rise to curved surfaces (STANTON, 1972). A free-growing mineral might develop its own crystal faces or convex outer surfaces due to surface tension. A younger mineral conforms to the crystal outlines of the older one. Convex interlocking surfaces are more abundant on the ealier

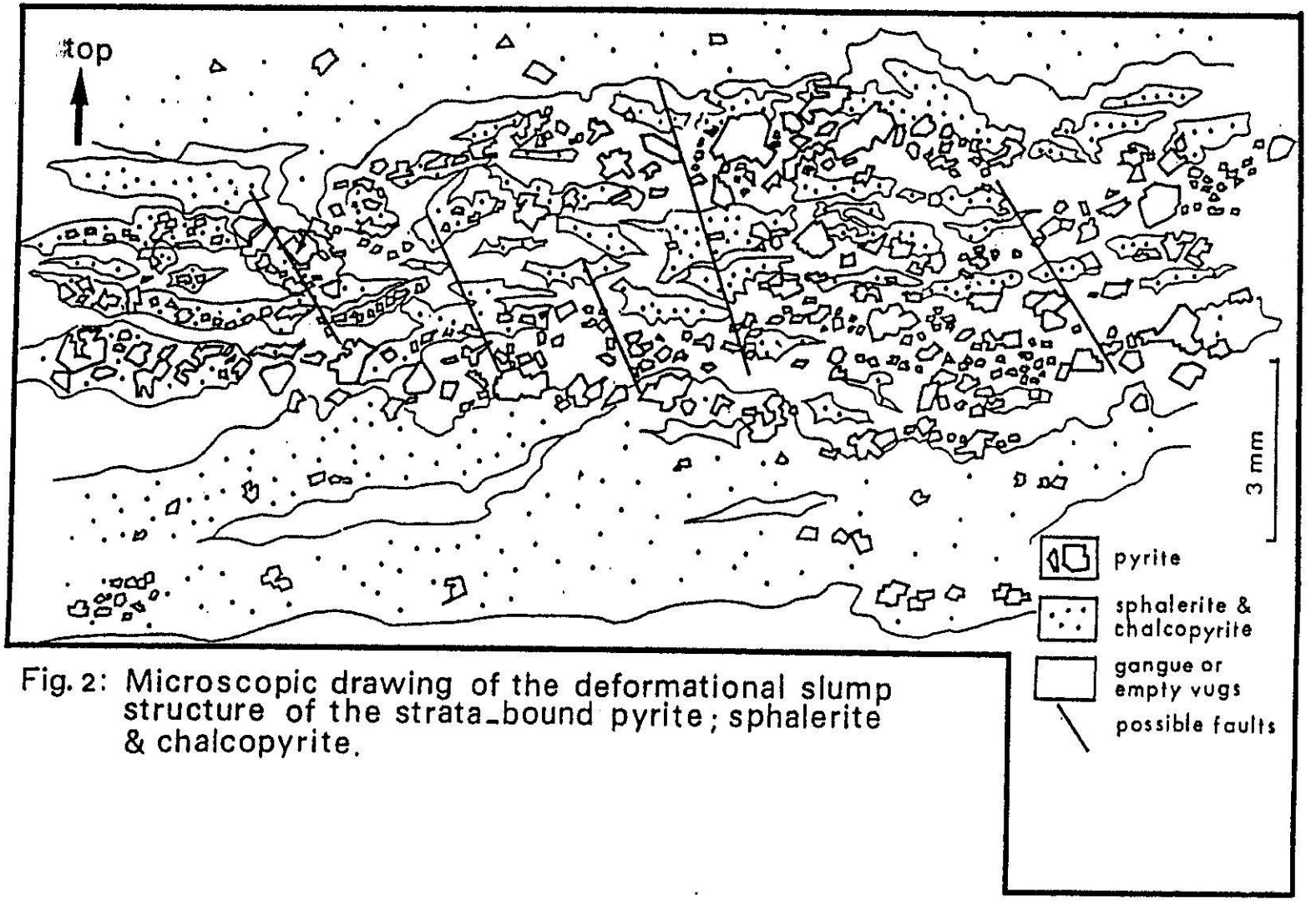

Fig. 2: Microscopic drawing of the deformational slump structure of the strata-bound pyrite; sphalerite & chalcopyrite.

minerals (BASTIN, 1953; EL BAZ, 1964, AMSTUTZ, 1965 and AMSTUTZ and GIGER, 1972). Therefore many intergrowth textures can be found to be overgrowths in free space.

In Group I (Pl. III) pyrite is always present in the interspaces between the clastic grains usually associated with calcite and carbonaceous matter (Pl. V, Fig.e). It occurs as individual crystals or clusters with well developed crystal faces against the other cement materials. Pyrite crystals are corroded or partially replaced by calcite (Pl. V, Fig.f) and included within epidote. Minute cubic pyrite crystals are enclosed within authigenic quartz and feldspar or enveloped by feldspar overgrowth (Pl. V, Fig.g). Sphalerite and chalcopyrite, if present, fill spaces and cracks in the pyrite crystals. The above picture indicates that pyrite and associated sulphides were deposited in the interspaces between the clastic grains of the tuffs together with or slightly before the deposition of calcite and colloidal silica, and of coarse prior to the formation of authigenic quartz, epidote and fledspar overgrowths.

The geometric relations observed in the different parageneses in the pyritic massive sulphide (Group II in Pl.III) are illustrated in Pl.VI. In the paragenesis pyrite sphalerite - chalcopyrite (Pl.VI,Fig.A),pyrite exhibits idiomorphic outlines against sphalerite and chalcopyrite (Pl.VII,Fig.a). Shpalerite and chalcopyrite fill spaces within the pyrite. Chalcopyrite occurs in two generations. The first generation (cp I) is intergrown with sphalerite forming dissiminated, lamellar and network intergrowth types (Pl.VII,Fig.b). The later generation of chalcopyrite (cp II) is usually interlocked with sphalerite. The sphalerite chalcopyrite interlocking exhibits mostly concave surfaces towards the former and convex surfaces towards the later (Pl.VII, Fic.c). Cp II fills strata-bound fractures in the sphalerite base (Pl.VII,Fig.d). The gangue (mainly chert) shows interbedded relation with sphalerite and cp II or fill spaces between the sulphides. In the paragenesis pyrite-sphalerite - chalcopyrite - galena (Pl.VI,Fig.B), pyrite appears to be the earliest mineral in the paragenetic sequence, where it shows idiomorphic outlines against the other minerals. Sphalerite and chalcopyrite I form a cement between the pyrite crystals and exhibit convex intergrowth surfaces towards chalcopyrite II and galena. Chalcopyrite II and galena show intercalated sequentional crystallization terminated with crystallization of chalcopyrite (Pl.VII, Fig.e). The gangue appears to be the last mineral in the paragenetic sequence where

it envelops the sulphides. In the paragensis sphalerite, galena, chalcopyrite, fahlore, bornite and covellite (Pl.VI,Fig.C and Pl.VI,Fig.f), pyrite was not detected and chalcopyrite I was not confidently recognized. Fahlore separated before chalcopyrite II which was followed by bornite and covellite. At present, we do not have enough information to decide whether bornite and covellite were primary minerals or were formed during secondary leaching or cementation processes.

The study of the interfaces between the different sulphide minerals and gangue revealed that they were deposited in a consistent order in all the different parageneses of the massive sulphide. The sequence of separation is given schematically on the following table:

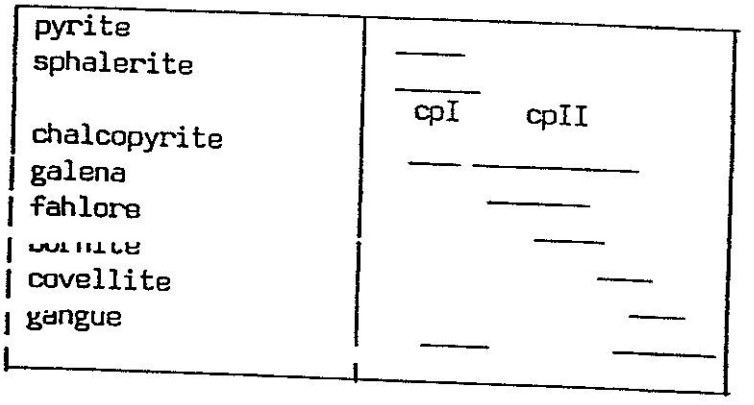

The essential sulphide minerals were formed before the crystallization of the gangue minerals, i.e., before final cementation and lithification of the enclosing tuffs. The physico-chemical conditions of the marine environment (and trapped connate water) seem to be the main factors controlling the sequence of sulphide mineral separation. The presence of carbonaceous matter indicates at least reducing conditions.

CONCLUSION

The sulphide minerals at Um Samiuki area are present in two main geometric forms, namely a) stratiform to strata-bound pyrite, with or without sphalerite and chalcopyrite, and b) stratiform to strata-bound pyritic massive sulphide consisting of Fe, Zn, Cu and Pb sulphide minerals. These forms are confined to the pyroclastic sediments of Late Proterozoic island arc association.

The study of the geometry of these forms in all scales revealed overall congruent relations between the fabrics of the sulphides and the primary and deformational textures of the host rocks. The microscopic geometric interfaces between the different sulphide minerals and gangue indicate primary crystallization and successive overgrowths between the clastic grains of the tuffs during burial and prior to final lithification, i.e. during the diagenetic evolution of the sediments. This high degree of congruency is a logic evidence suggesting synsedimentary origin of the sulphides.

The syndiagenetic sulphides and enclosing rocks apear to have been subjected to brecciation and hydrothermal alteration leading to the formation of talc and tremolite and mobilization of chalcopyrite.

ACKNOWLEDGEMENT

The authors wish to express their gratitude to Prof. Dr. S. EL GABY, Assiut University and Prof. Dr. M. EL SHARKAWI, Cairo University, for their useful discussions, reading the manuscript and constructive criticism.

REFERENCES

Amstutz, G.C. 1965 — A quantitative approach to paragenetic relations of ore minerals. Freiberger Forschungscheft, C. 186, 41-50.

Amstutz,G.C. and GiGer, H. 1972. Stereological methods applied to mineralogy, petrology, mineral deposits and ceramics. J. of Microscopy. V.95, Pt.1, 145-164.

Ball, J. 1912. — The geography and geology of South Eastern Desert, Egypt. Surv. Dept. Cairo, 394p.

Bastin, E. S. 1953 — Interpretation of ore textures. Geol. Soc. of America, Memoir 45, 101p.

El Baz, F. 1964. Petrology and mineralogy of certain portions of the Fredericktown deposits, Missouri. A case study of ore genesis in a layered sulphide deposit. Ph.D. Thesis, University of Missouri, U.S.A., 229p.

El Ramly, M. F. 1972. A new geological map for the basement rocks in the eastern and southewestern deserts of Egypt. Annals Geol. Surv. Egypt, II, 1-18.

El Shazly, E. M. 1975. Classification of Egyptian mineral deposits. Egypt. J. Geol. 1, 1-20.

El Shazly, E. M. 1964. On the classification of the Precambrian and other rocks of magmatic affiliation in Egypt. 24th Int. Geol. Cong. India., 10, 88-101.

El Shazly, E.M. and Afia, M.S. 1958. Geology of Samiuki deposit, Eastern Desert. J. Geol., 2, 25-42.

Fisher, R. V. and Schmincke, H. U. (1984). Pyroclastic rocks. Springer-Verlag, Berlin, New York, 473p.

Garson, N. S. and Shalaby, I.M. 1976. Precambrian Lower Paleozoic plate tectonics and metallogenesis in the Red Sea region. Spec. Pap. Geol. Assoc. Canada, V. 14, 573-596.

Hafez, A. and Shalaby, I.M. 1983. On the geochemical characteristics of the volcanic rocks at Umm Samiuki, Eastern Desert, Egypt. Egypt. J. Geol., 27, 1-2, 73-92.

Hume, W. F. 1937. Geology of Egypt V. II, 3, Survey Dept., Cairo, 689-990.

Hussein, A. A., Shalaby, I. M., Gad, M. A. and Rasmy, A. H. 1977. On the origin of Zn-Cu-Pb deposits at Um Samiuki, Eastern Desert. Geol. Surv. Cairo (unpublished report).

Jackson, M. L. 1958. Soil chemical analysis. Prentice-Hall, Inc. Englewood Cliffs, N.J., 205-226.

Lehne, R. W. and Amstutz, G. C. 1982. Sedimentary and diagenetic fabrics in the Cu-Pb-Zn-Ag Deposit of Colquijirca, Central Peru. In Ore genesis, the state of the art (Amstutz et al, ed.). Springer-Verlag, Berlin, 161-166.

Shulz, O. 1976 Typical and nontypical sedimentary ore fabrics. In handbook of strata-bound and stratiform ore deposits (Wolf, ed). Elsevier Scientific Publishing Company, Amsterdam, V.3, 295-338.

Searle, D. L., Carter, G. S. and Shalaby, I. M. 1976. A report in mineral exploration at Um Samiuki. UNDP. Internal Report, Cairo, 51p.

Searle, D.L., Carter, G.C., Shalaby,I.M. and Hussein,A.A. 1976 b. Ancient volcanism of island- arc type in the Eastern Desert of Egypt (Abs.), 25th Intern.Geol. Congress, Sydney, 1, sec. 2.

Shukri, N. M. and Mansour, M. S. 1980. Lithostratigraphy of UM Samiuki district, Eastern Desert, Egypt. Evolution and mineralization of the Arabian Nubian Shield,Jeddah, V.4, 83-93.

Soliman, F. A. M. 1981. Geological and geochemical studies on the mineralized area of Umm Samiuki, Eastern Desert, Egypt. M.Sc. Thesis, Cairo University, 92 p.

Stanton, R. L. 1972. Ore petrology. Mc Graw - Hill Book Company, 713 p.

Plate I

Fig. a : A photograph of Gebel Abu Hammamid, West of Wadi Um Samiuki, showing a stratified succession of volcaniclastics intercalated with volcanic sheets.

Fig. b : Pillow structure in basalt rock.

Fig. c : A polished slab of volcanic breccia.

Fig. d : Stratified distribution of calcareous nodules in cherty pyroclastic sediments.

Fig. e : A polished slab showing pyrite-rich laminae and bands (py) in pyroclastics.

Fig. f : A polsihed slab showing downward convexity of coarse grained tuff into dusty laminated tuffs.

PLATE I

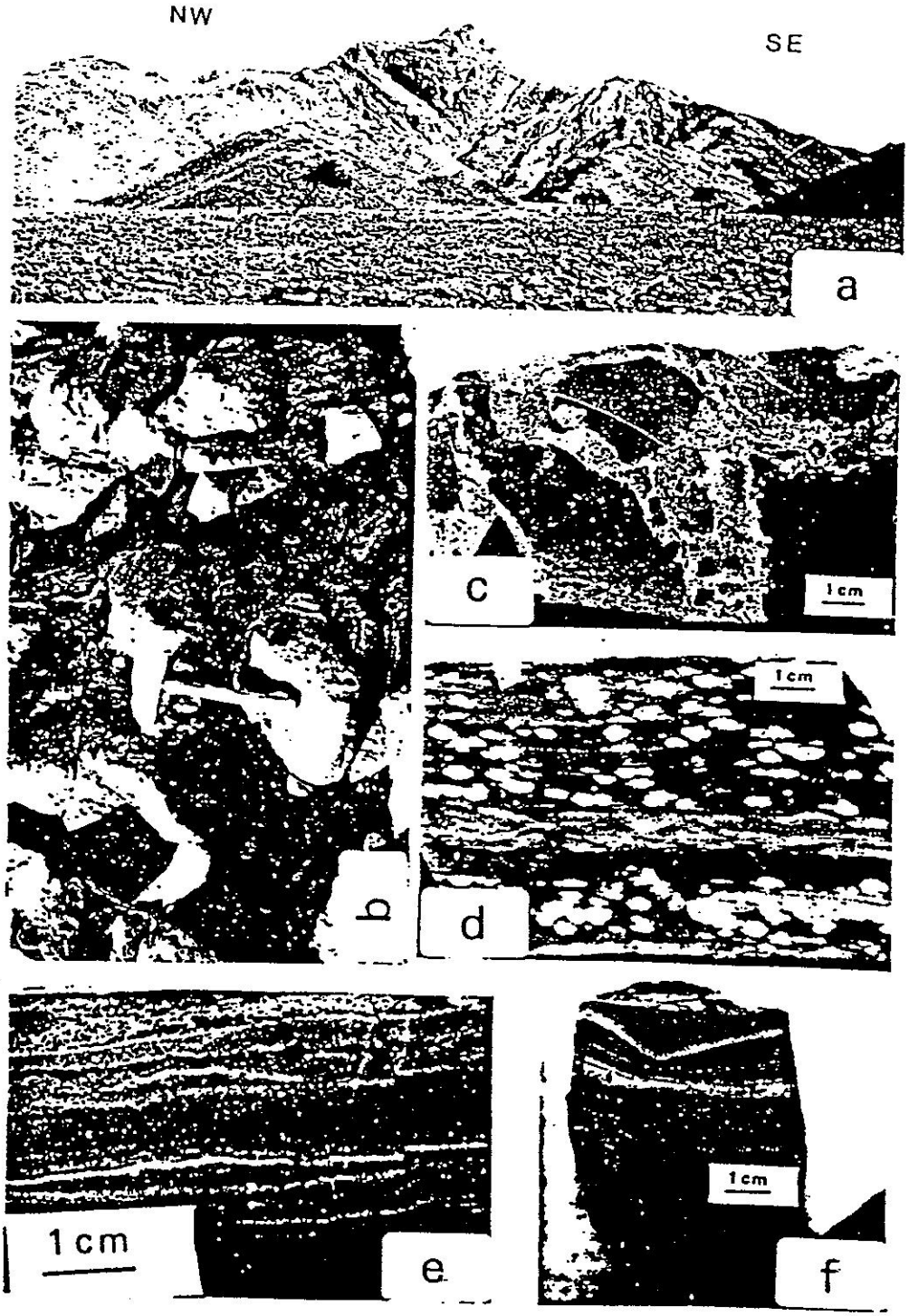

Plate II

Fig. a : A photomicrograph exhibiting downward convexity of medium-grained crystal lithic tuff (+ N, TS).

Fig. b : A photomicrograph showing geopetal loading sturcture developed by the projection of crystal ashs into underlaying cherty layer (// N, TS).

Fig. c : A photomicrograph showing geopetal loading formed by the projection of crystal tuff into underlaying carbonaceous clayey band (// N, TS).

Fig. d : A photomicrograph showing cut and fill sturcture in tuff (// N, TS).

Fig. e : A polished slab showing slump structure in laminated tuff.

Fig. f : A photomicrograph showing authigenic spherulitic growth of chalcedony (center of the photo) in the groundmass of coarse tuff (+ N, TS).

Fig. g : A photomicrograph showing authigenic quartz overgrowth (// N, TS).

Fig. h : A photomicrograph showing recrystallized of chert in the groundmass of tuff (+ N, TS.).

TS = Thin section.

PLATE II

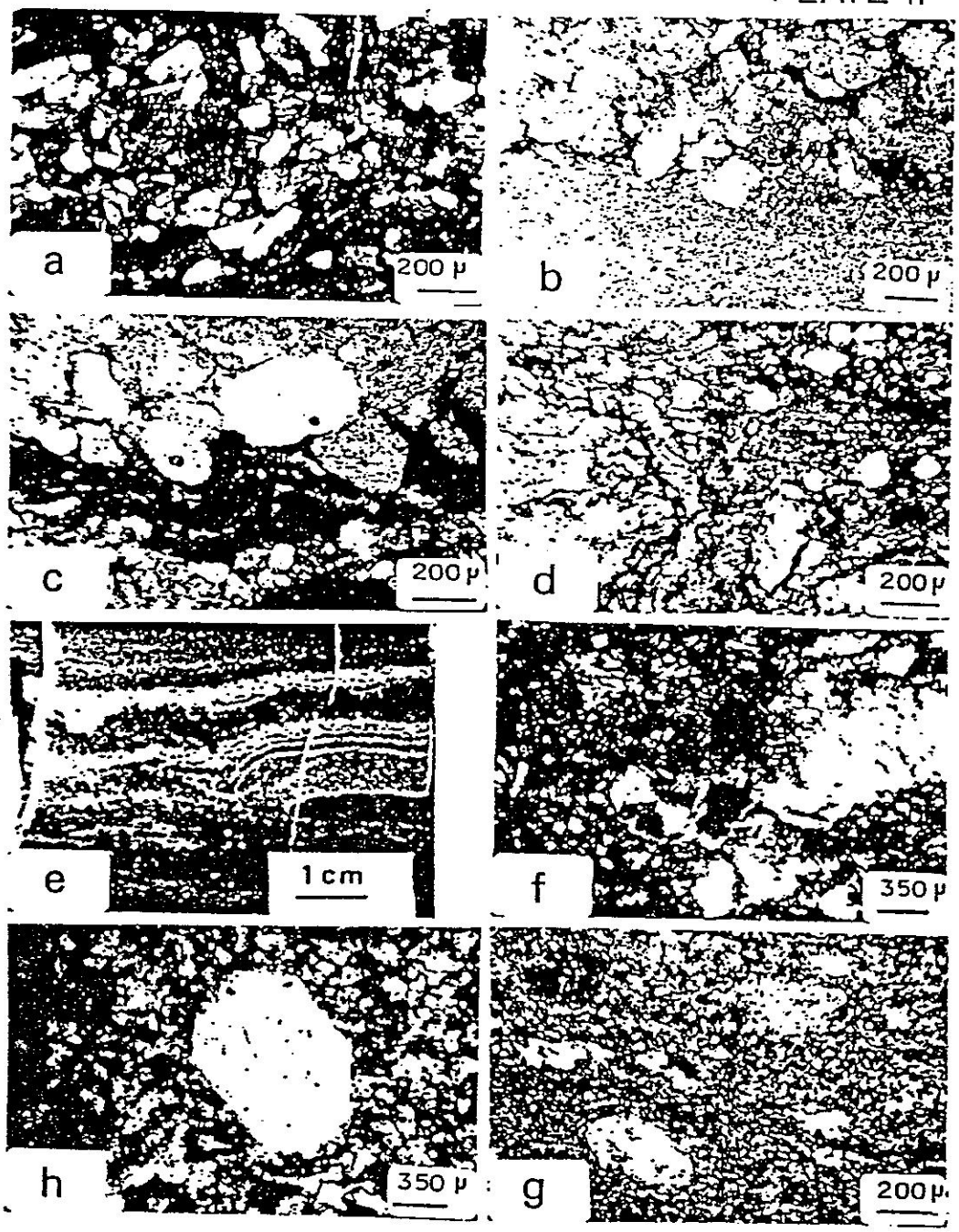

PLATE III

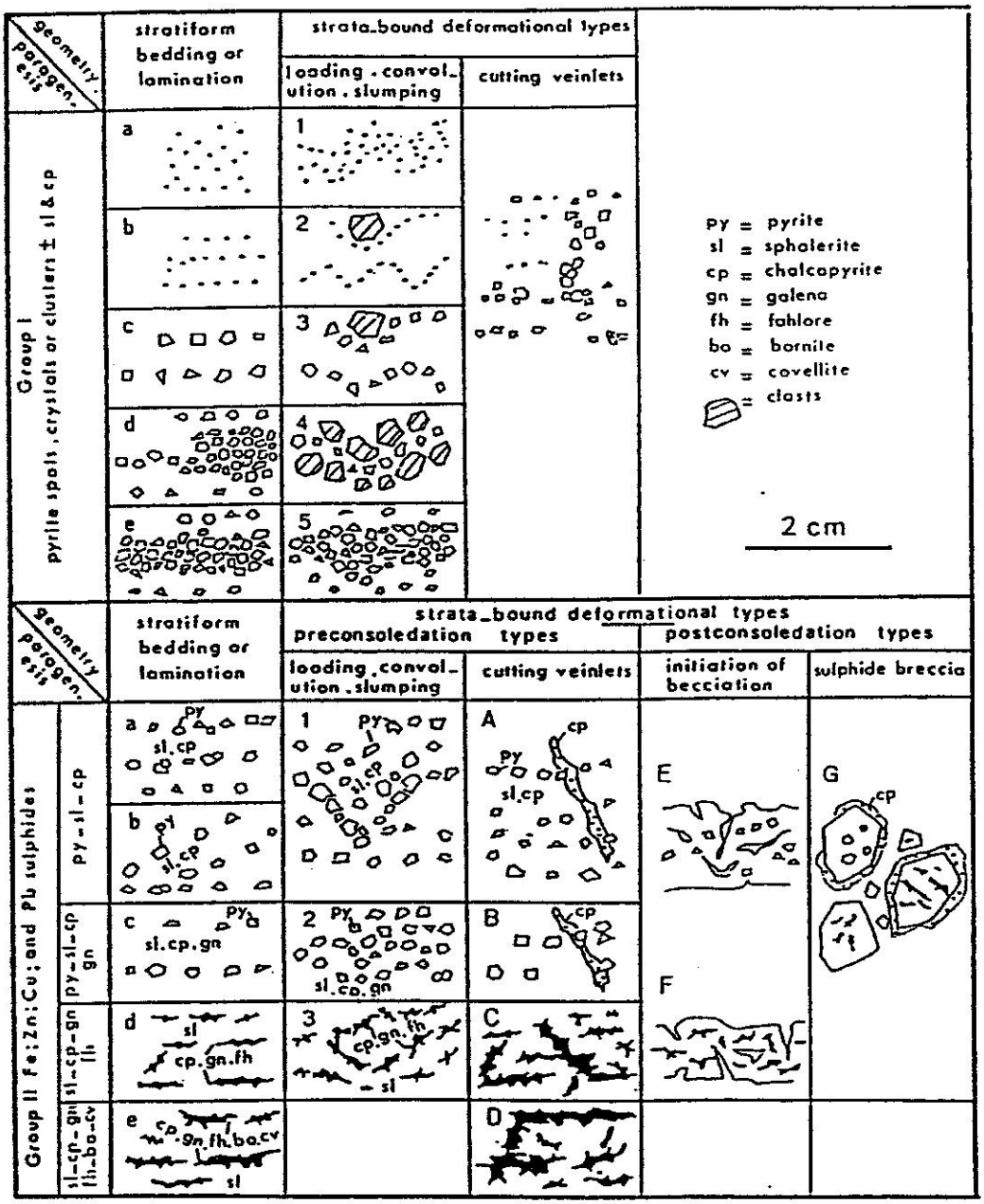

Schematic classification of the megascopic-microscopic geometric patterns of the Fe; Zn; Cu & Pb sulphides and their sedimentological approach (description in the text).

Plate IV

Representative examples (A, B, C) of banded and laminated pyroclastics showing primary and deformational sedimentary structures and some geometric distribution parterns of pyrite ± sphalerite and chalcopyrite.

Legend

1 = coarse-grained dacitic crystal tuff
2 = medium grained andesitic lithic crystal tuff
3 = medium grained andesitic crystal lithic tuff
4 = medium to fine grained andesitic crystal tuff
5 = dust tuff
6 = chert ± calcite
7 = calcareous material (silicieous in part)

py = pyrite ± sphalerite and chalcopyrite.

PLATE IV

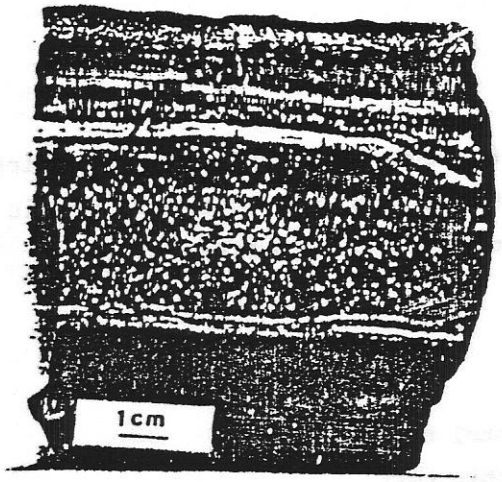

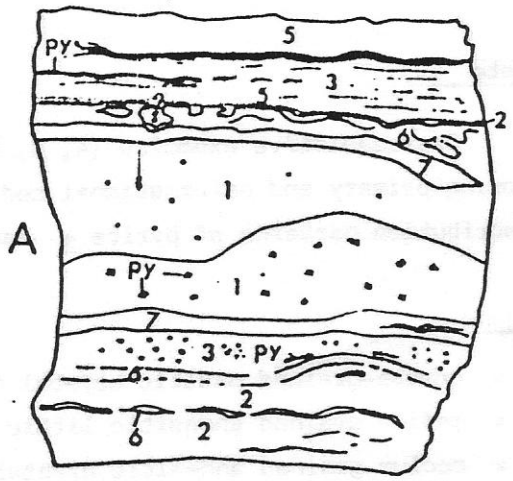

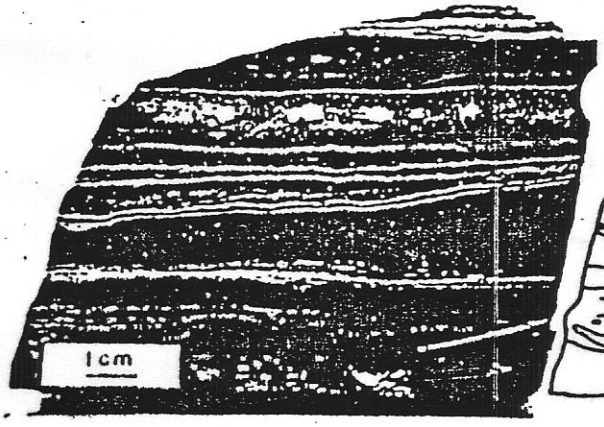

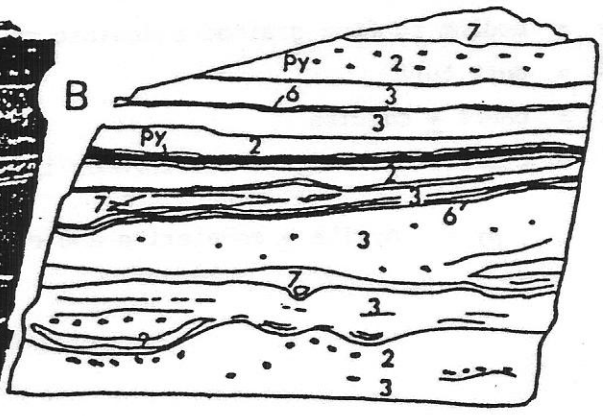

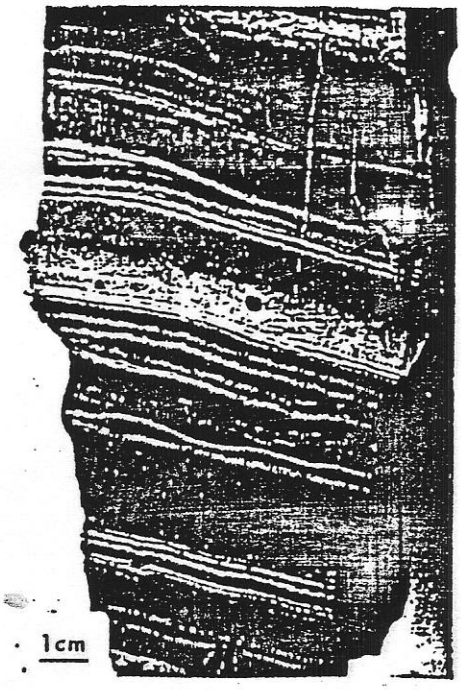

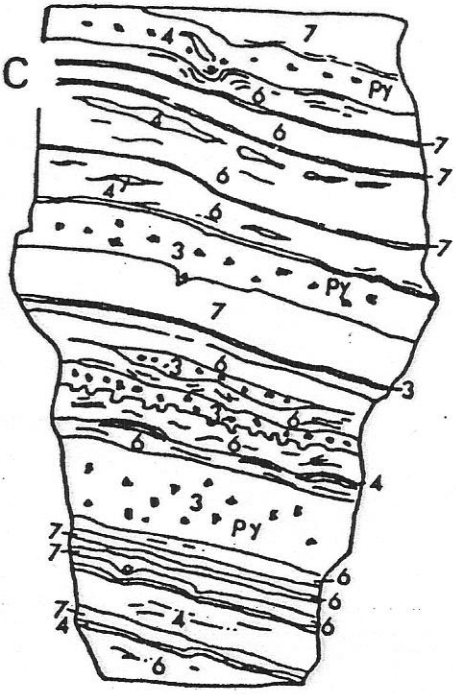

Plate V

Fig. a : A polished slab showing pyrite crystals (py) arranged in a undulated pattern.

Fig. b A photomicrograph showing geopetal loading structure developed by dropping of tuff clasts into pyrite (py) and sphalerite(sl) laminae ($\leq$ N, TS).

Fig. c : A polished slab of laminated sulphides characterized by stratified distribution of pyrite (white) in a sphalerite and chalcopyrite (grey) base. Note the strata-bound cross cutting veinlet of chalcopyrite (upper left corner of the photo)

Fig. d : A polished slab of breccia composed of sulphide volconic and tuff fragments cemented by talc and chalcopynite (cp).

Fig. e : A photomicrograph of crystal lithic tuff cemented by pyrite (black) ($\leq$ N, TS).

Fig. f : A photomicrograph showing a pyrite crystal (black) surrounded and partially replaced by calcite (white) ($\leq$ N, TS).

Fig. g : A photomicrograph showing authigenic albite in tuff over-growing and enclosing pyrite (lower left corner).

TS = Thin Section.

PLATE V

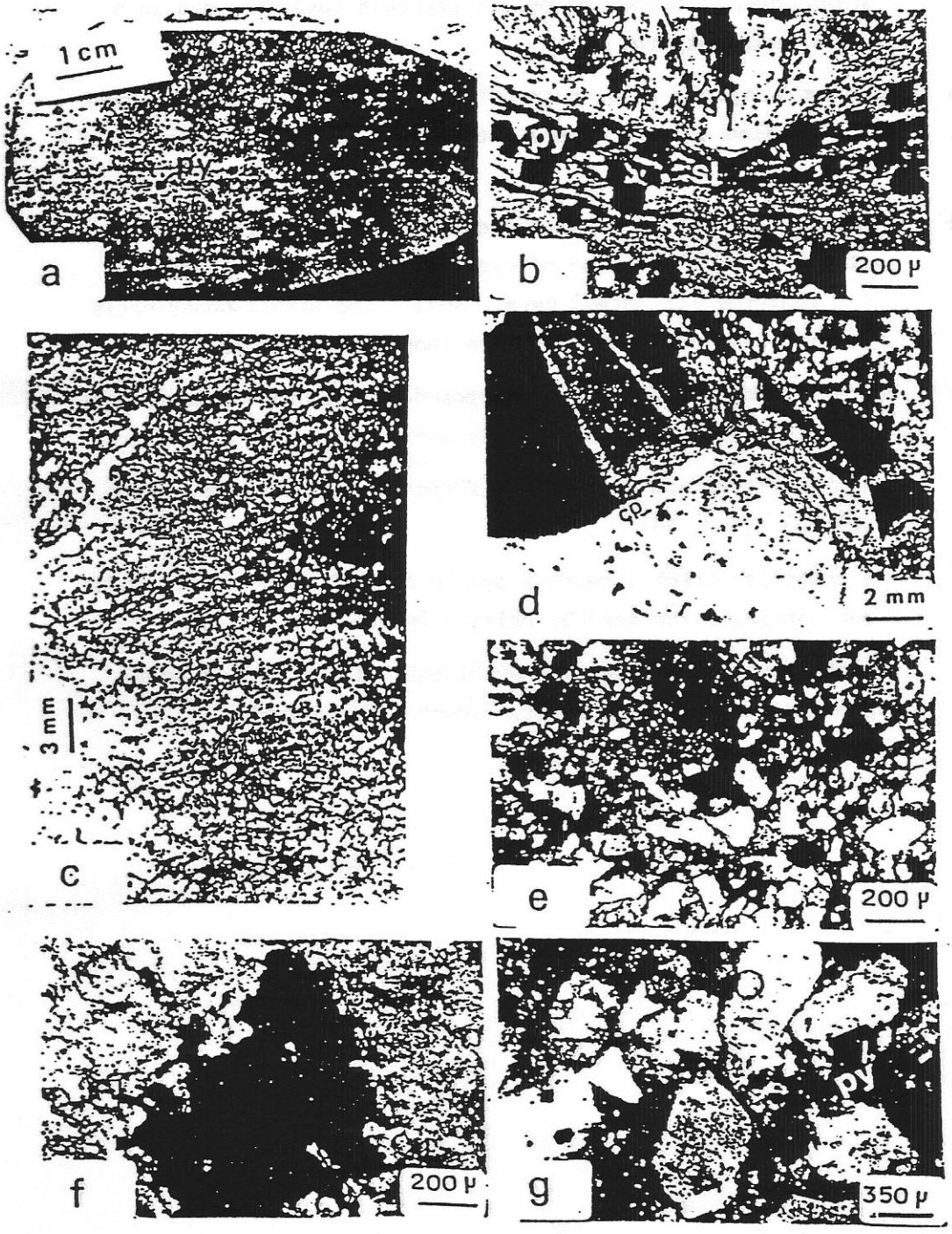

PLATE VI

py = pyrite ; sl = sphalerite; cp = chalcopyrite;
gn = galena; fh = fahlore; bo = bornite;
cv = covellite ; gg = gangue; # = locked to.

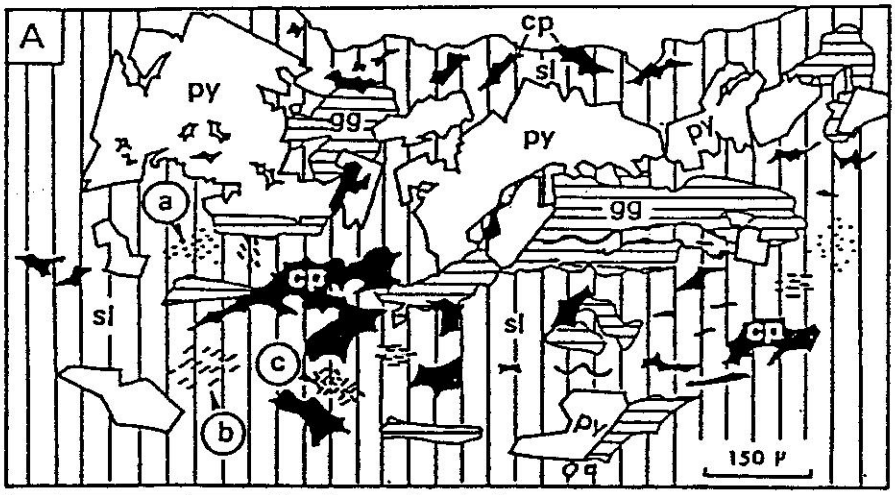

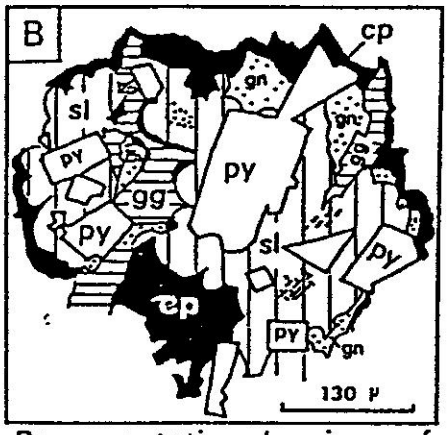

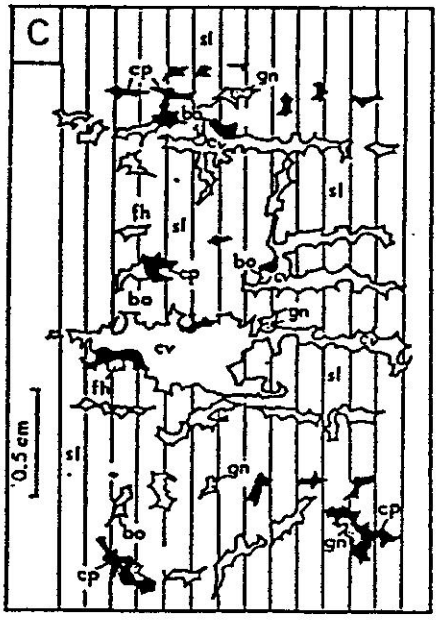

Representative drawings of the microscopic geometric interfaces of the sulphides

Locked possibilities and their intergrowth surfaces

Fig.(A) py_sl_cp

py # sl	py shows euhedral outlines against sl & cpII disseminated(a); lamellae(b) & network(c) intergrowths
py # cpII	
sl # cpI	
sl # cpII	concave surfaces towards sl

Fig.(B) py_sl_gn_cp

py # sl	py shows euhedral outlines against sl ; cpII & gn types a;b & c of Fig. A
py # cpII	
py # gn	
sl # cpI	
sl # gn	concave surfaces towards sl
sl # cpII	〃 〃 〃 〃
gn # cpII	〃 〃 〃 gn
	and vica versa

Fig.(C) sl_gn_cp_fh_bo_cv

sl # gn	concave	surfaces	towards	sl
sl # cp	〃	〃	〃	sl
sl # cv	〃	〃	〃	sl
sl # fh	〃	〃	〃	sl
sl # bo	〃	〃	〃	sl
cp # cv	〃	〃	〃	cp
cp # bo	〃	〃	〃	cp
cp # gn	〃	〃	〃	gn
cp # fh	〃	〃	〃	fh
gn # bo	〃	〃	〃	gn
gn # cv	〃	〃	〃	gn
cv # fh	〃	〃	〃	fh
cv # bo	〃	〃	〃	bo

Plate VII

Fig. a : A photomicrograph showing idiomorphic pyrite (py) and concave-convex relation between sphalerite (Sl) and chalcopyrite (cp), (≂N, PS, air).

Fig. b : A photomicrograph showing dissiminated, lamillae and network intergrowths between sphalerite (grey) and chalcopyrite I (white), (≂N, PS, air).

Fig. c : A photomicrograph showing interlocking relation between sphalerite (grey) and chalcopyrite II (white), (≂N, PS, air).

Fig. d : A photomicrograph showing a strata-bound veinlet of chalcopyrite white cutting across sphalerite (grey), (≂N, PS, air).

Fig. e : A photomicrograph showing interlocking relation between pyrite (cubes), sphalerite (dark grey),galena (light grey) and chalcopyrite (white), (≂N, PS, air).

Fig. f : A photomicrograph showing overgrowth relations of sphalerite (grey), chalcopyrite (white) and covellite (dark grey), (≂N, PS, air).

PS = Polished section.

PLATE VII